Mixed Micelles of Triton X-100, Sodium Dodecyl Dioxyethylene Sulfate, and Synperonic L61 Investigated by NOESY and Diffusion Ordered NMR Spectroscopy

Pavletta S. Denkova,*,†,‡ Luk Van Lokeren,† and Rudolph Willem†

Vrije Universiteit Brussel, High Resolution NMR Centre (HNMR), Department of Materials and Chemistry (MACH), Pleinlaan 2, B-1050 Brussels, Belgium, and NMR Laboratory, Institute of Organic Chemistry with Centre of Phytochemistry, Bulgarian Academy of Sciences, Acad. G. Bontchev Str., Bl.9, 1113 Sofia, Bulgaria

Received: November 27, 2008; Revised Manuscript Received: March 24, 2009

Mixed micelles formed from nonionic surfactant Triton X-100 (TX100), anionic surfactant sodium dodecyl dioxyethylene sulfate (SDP2S), and triblock copolymer Synperonic L61 (SL61) were investigated by ^{1}H NMR spectroscopy. The size and shape of the aggregates were determined by diffusion ordered NMR spectroscopy (DOSY), while 2D nuclear Overhauser enhanced spectroscopy (NOESY) NMR was used to study the mutual spatial arrangement of the surfactant molecules in the aggregated state. An average micellar hydrodynamic radius of 3.6 nm, slightly increasing upon increasing TX100 molar fraction, was found for the mixed systems without additives. Addition of SL61 to the mixed micellar systems results in a slight increase of micellar radii. In the presence of $AlCl_3$, an increase of TX100/SDP2S micellar sizes from 4 to 10 nm was found when increasing the SDP2S molar fraction. The mixed TX100/SDP2S micelles in the presence of both $AlCl_3$ and polymer SL61 are almost spherical, with a radius of 4.5 nm. 2D NOESY data reveal that, as the individual TX100 micelles, mixed TX100/SDP2S and TX100/SDP2S/SL61/$AlCl_3$ micelles also have a multilayer structure, with partially overlapping internal and external layers of TX100 molecules. In these mixed micelles, the SDP2S molecules are located at the level of the external layer of TX100 molecules, whereas the SL61 polymer is partially incorporated inside of the micellar core.

1. Introduction

Mixed micellar systems of ionic and nonionic surfactants or surfactant−polymer formulations have wide practical importance in various biological, technological, and industrial fields of applications such as detergents, cosmetics, drug delivery systems, paints, etc. Mixed micelles are more flexible with regard to their properties and areas of application, since their functionality can be fine-tuned by composition modulation. The unremitting interest in mixed nonionic/ionic surfactant and surfactant−polymer solutions stems also from their higher capacity to solubilize water insoluble compounds (hydrophobic substances, hydrocarbons, etc.) because of their synergic performance.[1−4]

The size and shape of micelles and their supramolecular structure are important characteristics of surfactant systems affecting their properties and application areas. The type of interactions, various physicochemical properties and structure of binary nonionic/ionic surfactant or surfactant/polymer mixtures were previously investigated using a whole range of different techniques, like dynamic light scattering, viscosity measurements, X-ray scattering, and NMR spectroscopy.[5−17] Detailed structural information about more complex ternary systems, consisting of two surfactants and a polymer, frequently used in industrial applications, remains, however, quite scarce. Mixtures of one ionic and one nonionic surfactant in the presence of oppositely charged polyelectrolyte have been studied by Dubin et al.[18−20] Neutron reflectivity and surface tension data have been used to investigate the adsorption behavior of a mixture composed of, for instance, sodium dodecyl sulfate (SDS) and hexaethylene glycol monododecyl ether ($C_{12}E_6$) at the water/air interface, in the presence of the cationic dimethyldiallylammonium chloride−acrylamide copolymer.[21,22] Interactions and association behavior of components in mixtures of poly(ethylene oxide) and two surfactants, SDS and sodium decyl phosphate, have been studied by conductivity measurements.[23] Recently, the interactions in ternary aggregates between polyvinylpyrrolidone (PVP), the anionic SDS surfactant, and, as a third component, the nonionic surfactant (pentaethylene glycol monodecyl ether, $C_{10}E_5$) or the zwitterionic surfactant (lauryl amido propyl betaine, LAPB) have been investigated by diffusion NMR.[24] Söderman and Stilbs[25] reviewed full NMR based strategies combining diffusion ordered spectroscopy (DOSY) and nuclear Overhauser enhanced spectroscopy (NOESY and/or HOESY) to elucidate molecular aggregation. Jérôme et al.[26,27] adopted this strategy for a binary surfactant mixture with an anionic surfactant, SDS, and a nonionic one, the block copolymer poly(ethylene oxide)-*b*-poly(ε-caprolactone), to demonstrate interaction without establishing explicit spatial arrangements. Recently, the influence of block copolymers on the solubilization kinetics of triglycerides into individual and mixed micellar solutions containing penta- or hexaethylene glycol monododecyl ether as nonionic surfactants and sodium dodecyl sulfate (SDS) or sodium dodecyl dioxyethylene sulfate (SDP2S) as anionic surfactants has been extensively investigated.[28] This investigation demonstrated that the complex system containing both nonionic and ionic surfactants together in the presence of both the polymer and the electrolyte has a higher oil solubilization rate and capacity when compared to the individual or binary systems. These data show that while the kinetics of oil solubilization depends on the surfactant composition, the

* To whom correspondence should be addressed. E-mail: psd@orgchm.bas.bg. Phone: +359 (2) 9606 172. Fax: +359 (2) 870 02 25.
† Vrije Universiteit Brussel.
‡ Bulgarian Academy of Sciences.

10.1021/jp8104369 CCC: $40.75
Published on Web 04/22/2009

solubilization capacity is mainly related to the specific micellar structure, which is not—to the best of our knowledge—unraveled so far.

The present investigation focuses on spatial arrangements of surfactant molecules within mixed micelles in a ternary system composed of the anionic surfactant SDP2S, the nonionic surfactant *p-tert*-octylphenol-polyoxyethylene ether with averaged 9.5 oxyetylene groups (Triton X-100, TX100) and the triblock copolymer of type polyethyleneoxide−polypropyleneoxide−polyethyleneoxide, Synperonic L61 (SL61; PEO_n−PPO_m−PEO_n, $n \approx 2.5$, $m \approx 30$). The size and shape of surfactant micelles were determined by DOSY,[29−32] while the structure of the aggregates was investigated by 2D NOESY.[33]

In the present study, we unravel the relative arrangement of the component molecules in the ternary TX100/SDP2S/SL61 micellar system in the presence of $AlCl_3$ and propose a detailed micellar structure, illustrating the capacity, added value, and complementarity of both NMR techniques for a comprehensive structural investigation of complex multicomponent micellar mixtures. In the ^{1}H NMR spectrum of mixed solutions, the signals of aromatic and terminal methyl protons from the *p-tert*-octyl moiety of TX100 do not overlap with signals from the two other components. Thus, these resonances can be used as probes to gain information about the relative arrangement of the hydrophobic parts of the constituent surfactant molecules in the interior of their mixed micelles.

2. Experimental Section

2.1. Materials. *p-tert-Octyl-phenyl-polyoxyethylene-(9.5) glycol* (Triton X-100 (TX100), Sigma) with an average of 9.5 oxyethylene units per molecule, $C_8H_{17}C_6H_4(OCH_2CH_2)_{9.5}OH$ (MW = 646), sodium dodecyl dioxyethylene sulfate (SDP2S, Empicol ESB70, aqueous solution of 70% active substance), $CH_3(CH_2)_{11}(OCH_2CH_2)_2OSO_3Na$ (MW = 376), and triblock copolymer $(C_2H_4O)_{2.5}(C_3H_7O)_{30}(C_2H_4O)_{2.5}$ (ICI, Synperonic PE/L61, (SL61), MW $\approx$ 2100) were used as purchased.

All solutions were prepared with D_2O (99.95%, Aldrich) and equilibrated for 48 h at room temperature prior to the measurements. Anhydrous $AlCl_3$ (Merck) was used to prepare solutions with electrolyte.

2.2. Methods. All diffusion NMR measurements were performed at 300 K on a Bruker Avance DRX 250 NMR spectrometer equipped with a high gradient diffusion probe Diff 30. NOESY spectra were measured on the same spectrometer using a QNP probe.

DOSY Spectra. The DOSY spectra were acquired with the *ledbpgp2s* pulse program from Bruker Topspin software, adapted to include a water presaturation cycle. All spectra were recorded with 16 K time domain data points in t_2 dimension and 32 t_1 increments, with 16 transients each and a relaxation delay of 3 s.

The experimental parameters for diffusion measurements were optimized according to a procedure described previously.[34]

All measurements were performed with a compromise diffusion delay Δ of 100 ms in order to keep the relaxation contribution to the signal attenuation constant for all samples. The gradient pulse length δ was 1 ms except for samples with very low D values, where it was 1.6 ms in order to ensure full signal attenuation. The gradient pulse strength G was varied in 32 linear steps in the interval from 2 to 45% of the maximum gradient output of the gradient unit (12 T/m) and up to 65% for samples with higher concentration. The spectra were first processed in the F2 dimension by standard Fourier transform with 2 K data points and sine squared window function (qsine, ssb = 2). The data set representing the diffusion determined signal attenuation as a function of the NMR scattering vector q^2 ($q = \gamma\delta G$) was subjected to inverse Laplace transform using the MaxEnt method implemented in the GIFADOSYm[35] software package integrated in Topspin, as explained previously.[34]

NOESY Spectra. The 2D NOESY spectra were recorded with the standard Bruker program *noesygptp* in the phase-sensitive mode, using States−time-proportional phase incremention (States−TPPI) and sine shaped gradient pulses during the mixing period. The spectra were recorded with a spectral width of 2000 Hz, 1 K data points in t_2 time domain and 256 t_1 increments with 32 transients each, and a relaxation delay of 3 s. The spectra were recorded for each sample with at least seven different mixing times ranging from 5 to 600 ms in order to ensure optimal discrimination between actual NOE contacts and spin-diffusion cross-peaks, and to determine accurately the mixing time range where the initial rate approximation holds. A sine window function (ssb = 2) and zero-filling were applied in both dimensions prior to Fourier transformation, to give 2048 × 2048 data matrices in the frequency domain with 0.98 Hz/pt of digital resolution.

3. Results and Discussion

Figure 1 shows the chemical structures of the three substances, the respective structure fragment labeling, and their corresponding NMR spectra, from which the resonance assignment was performed.

Mixed solutions of TX100 and SDP2S were studied first in the absence of electrolyte and polymer in order to investigate systematically the influence of additives on their micellar properties.

3.1. Mixed TX100/SDP2S Micelles in the Absence of Electrolyte and Polymer. A series of solutions with constant total surfactant concentration of 12 mM but variable molar ratios of the two surfactants TX100 and SDP2S was investigated. This concentration is far above the critical micelle concentration (CMC) value of each surfactant, 0.25 mM for TX100 and 0.8 mM for SDP2S in the absence of additives.[34] Figure 2 represents a plot of the measured diffusion coefficients in mixtures of TX100 (full dots) and SDP2S (full triangles) as a function of the molar concentrations. For comparison, the diffusion data, as obtained from DOSY data for the corresponding individual micellar solutions in the same concentration range, are given with open symbols.[34] The results show that the D_{mix} values of the two surfactants in mixed solutions are very close, which is an indication of mixed micelles rather than a mixture of individual micelles of the two surfactants. The diffusion coefficients of TX100 in mixed micelles were determined from the methyl group resonances of the *p-tert*-octyl-phenyl fragment at 0.62 and 1.2 ppm, the aromatic proton resonances at 7.1 and 6.7 ppm, and the resonances at 3.9 and 3.7 ppm from the $-O-CH_2-CH_2-O-$ group directly bound to the aromatic ring. As seen from Figure 2, the D_{mix} values of TX100 show a minor dependence on solution composition, decreasing slightly but noticeably from 5.99×10^{-11} to 5.48×10^{-11} m^2/s (slope = -0.085 ± 0.035) upon increasing the TX100 molar fraction from 3 to 9 mM and approach the value for the individual TX100 micelles at 12 mM (5.13×10^{-11} m^2/s).

The diffusion coefficient of SDP2S in mixed solutions follows a parallel trend to that of TX100, decreasing slightly from 7.58×10^{-11} to 6.46×10^{-11} m^2/s upon decreasing the SDP2S molar concentration from 9 to 3 mM. One possible explanation to the systematically higher D_{mix} values of SDP2S as compared to

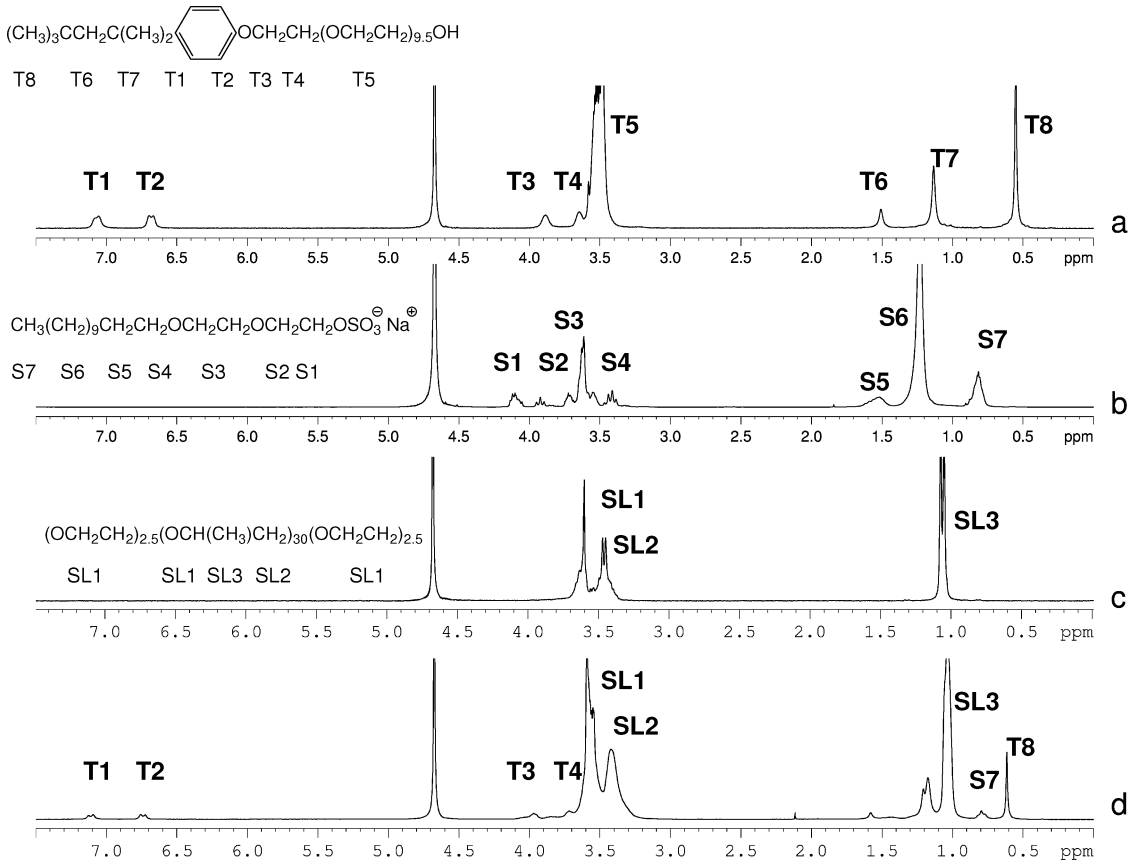

Figure 1. Molecular structures of TX100 (a), SDP2S (b), and SL61 (c), with their proton spectra (spectrum with resonances T, TX100; resonances S, SDP2S; resonances SL, SL61) displaying the proton resonance assignment using the labeling shown in the structures. Part d represents the spectrum of the mixed TX100/SDP2S/SL61 solution.

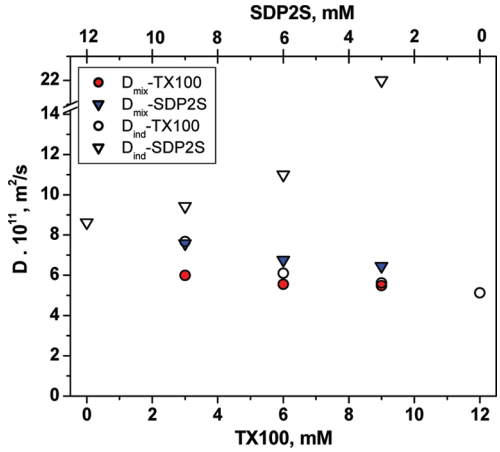

Figure 2. Diffusion coefficients as a function of surfactant molar concentration for the TX100/SDP2S system without any additive.

TX100 can be related to different contributions of the monomers of the two surfactants, since above the CMC there is usually a fast exchange of molecules between the monomeric and micellar states, resulting in a population weighted average of the monomer and micellar diffusion coefficients. Thus, the diffusion coefficient of TX100 molecules in the monomeric state was previously found to be 2.88×10^{-10} m^2/s, while that of SDP2S is much higher, 4.27×10^{-10} m^2/s.[34] The difference between D_{mix}(SDP2S) and D_{mix}(TX100) increases from 18 to 27% upon increasing the SDP2S concentration from 3 to 9 mM. This result along with the almost constant value of D_{mix}(TX100) as a function of its molar concentration indicates that, at higher SDP2S molar concentration, the molar fraction of the two surfactants in their mixture at equilibrium differs from their analytical input fraction. It also implies possible changes of micellar composition toward an increase of SDP2S monomer molar fraction upon increasing its molar concentration, while the nonionic monomer molar fraction stays almost constant at different molar ratios of the two surfactants. Similar results were obtained with 1D PGSE NMR experiments for mixed micelles formed by anionic/nonionic surfactants, like SDS/pentaethylene glycol monodecyl ether, for instance, which display some structural similarity with our system.[24,36]

The SDP2S diffusion coefficients, D_{mix}(SDP2S), decrease upon decreasing its molar fraction, which is in the opposite direction to the evolution of the diffusion coefficient in pure SDP2S solutions with the same surfactant concentration (see open triangles in Figure 2). The difference between the two values decreases from 66 to about 30% while increasing the SDP2S concentration in the mixed SDP2S/TX100 solution from 3 to 9 mM. This result shows that D_{mix}(SDP2S) remains much lower than D_{ind}(SDP2S), even in the mixed solution with the highest SDP2S molar fraction. These findings indicate that even in the presence of a very low fraction of nonionic surfactant there is a strong interaction between the two types of surfactant molecules.

Using the *Stokes−Einstein* equation

$$D = \frac{kT}{6\pi\eta R_h} \quad (1)$$

where η is the viscosity of D_2O, 1.0511 cP at 300 K (NIST), a micellar hydrodynamic radius, R_h, of 3.6 nm was found for the mixed SDP2S/TX100 micelles.

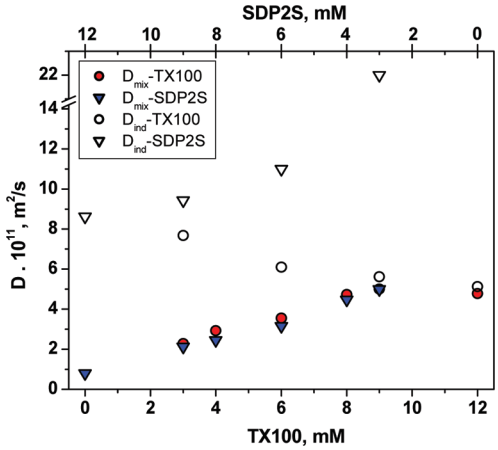

Figure 3. Diffusion coefficients as a function of surfactant molar concentration for the TX100/SDP2S system in the presence of 12 mM $AlCl_3$.

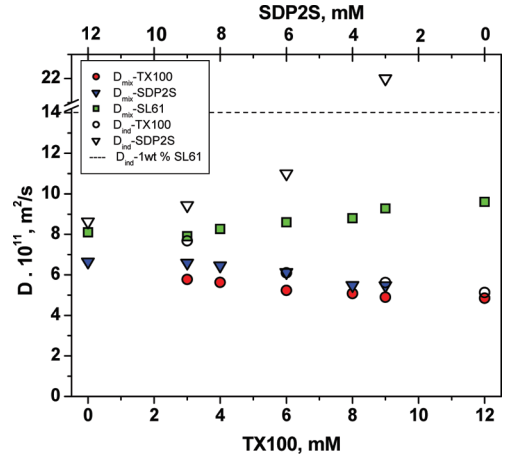

Figure 4. Diffusion coefficients as a function of surfactant molar concentration for the TX100/SDP2S system in the presence of 1 wt % Synperonic L61.

3.2. Mixed TX100/SDP2S Micelles in the Presence of $AlCl_3$. It is well-known that multivalent ions can dramatically change the properties of surfactant solutions, influencing the size, shape, and solubilization capacity of the micelles.[37,38] Figure 3 represents the measured diffusion coefficients of TX100 (full dots) and SDP2S (full triangles) in the presence of 12 mM $AlCl_3$, at an equimolar constant total surfactant concentration of 12 mM, but with different molar fractions of the two surfactants in mixed solutions. In this case, the diffusion coefficients of the two surfactants are equal within the limits of the experimental error and decrease upon increasing SDP2S molar concentration, tending to the value of pure SDP2S micellar solution at 12 mM in the presence of $AlCl_3$. The measured diffusion coefficients are systematically lower (by a factor of 4.3) in the presence of electrolyte than those of the pure SDP2S solutions (open triangles) without any additive but follow the same trend. By contrast to the situation in the absence of the salt, the TX100 diffusive behavior now mimics that of SDP2S. These observations indicate that in the presence of electrolyte the mixed micelles are larger and their size increases upon increasing SDP2S molar concentration. These results imply that in the presence of electrolyte the determinant factor for mixed micelle formation and micellar size/shape is the anionic surfactant, in contrast with the situation without electrolyte, where the TX100 surfactant was found to be the dominant factor. The micellar hydrodynamic radius, R_h, calculated using eq 1 increases from 4.2 to 9.8 nm upon increasing SDP2S molar concentration, indicating possible sphere-to-rod shape transition.[37,38] The almost identical D_{mix} values measured for the two surfactants show that the actual micellar equilibrium composition reflects the analytical solution composition and that the monomer concentration is negligibly low, in agreement with the much lower CMC value of SDP2S in the presence of multivalent ions.[37,38]

3.3. Mixed TX100/SDP2S Micelles in the Presence of SL61. Previous studies show that in many systems the addition of triblock copolymers to micellar solutions promotes oil solubilization.[28] Accordingly, to investigate the influence of polymer on micellar properties, the mixed TX100/SDP2S solutions were studied in the presence of SL61. The total surfactant concentration was again maintained constant at 12 mM, with variable surfactant molar fractions and in the presence of 5 mM (1 wt %) SL61. Figure 4 displays the diffusion coefficients of the two surfactants and the polymer as a function of the solution composition. The results are very close to those for the system in the absence of polymer. The measured diffusion coefficients of the two surfactants slightly decrease upon increasing the TX100 molar fraction from 5.77×10^{-11} to 4.90×10^{-11} m^2/s for TX100 and from 6.59×10^{-11} to 5.47×10^{-11} m^2/s for SDP2S. The D_{mix} values are again systematically higher for SDP2S than for TX100, which indicates a stronger contribution from SDP2S monomers. Comparison of Figures 2 and 4 shows that the diffusion data for TX100 are very close in the absence and in the presence of the polymer, while SDP2S diffusion coefficients are significantly lower in the presence of SL61. Lower D_{mix}(SDP2S) values in the presence of polymer suggest that SL61 interacts more strongly with the anionic surfactant[14,24] and decreases the relative fraction of SDP2S monomers in the equilibrium with aggregates of polymer/mixed micelles. Other evidence is the decreasing diffusion coefficient of the polymer in the mixture (Figure 4, squares) from 9.27×10^{-11} to 7.91×10^{-11} m^2/s with increasing SDP2S molar fraction. These values are much lower than the SL61 diffusion coefficient in its pure solution at the same concentration, which is 14.1×10^{-11} m^2/s (Figure 4, dashed line). The higher D_{mix}(SL61) value than the D_{mix} values for the two surfactants means that the polymer is only partially aggregated with the micelles and that there is a significant fraction of free polymer molecules. The decrease of D_{mix}(SL61) upon increasing SDP2S molar fraction is additional proof that the interaction between the polymer and the anionic surfactant is stronger, thus ruling out polymer aggregation.

In summary, the addition of triblock copolymer SL61 leads to a slight increase of micellar size, but the presence of the polymer does not change the characteristics of the mixed TX100/SDP2S micelles and has a relatively small influence on their size and shape.

3.4. Mixed TX100/SDP2S Micelles in the Presence of SL61 and $AlCl_3$. The diffusion coefficients of the ternary TX100/SDP2S/SL61 system in the presence of 12 mM $AlCl_3$ are displayed in Figure 5. The diffusion coefficients of the two surfactants are identical within the limits of the experimental error, averaging at 4.67×10^{-11} m^2/s. Comparison between Figures 3 and 5 reveals that, unlike the TX100/SDP2S/$AlCl_3$ system without SL61, in the presence of polymer, surfactant diffusion coefficients do not decrease upon increasing SDP2S molar fraction. These observations are explained if it is assumed that the polymer interacts with the anionic surfactant, breaking the long rod-like micelles formed upon increasing the SDP2S molar fraction to smaller spherical aggregates. In the presence

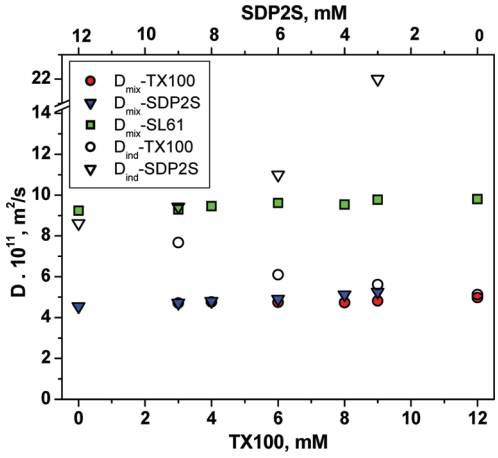

Figure 5. Diffusion coefficients as a function of surfactant molar concentration for the ternary TX100/SDP2S/SL61 system in the presence of 12 mM $AlCl_3$.

of both polymer and electrolyte, the mixed TX100/SDP2S micelles are spherical, relatively small, with an average hydrodynamic radius, R_h, of 4.5 nm, and their size and shape do not depend on the surfactant molar ratio. Identical D_{mix} values of the two surfactants also imply that the monomer fraction is negligible and the micellar composition reflects the initial analytical solution composition. The diffusion coefficient of SL61 does not depend significantly on the surfactant molar ratio and averages at 9.53×10^{-11} m^2/s, which is higher than the SL61 diffusion coefficients measured in the absence of electrolyte but much lower than the one for pure SL61 solution at the same concentration. The quantity of the polymer incorporated into the micelles is estimated from the following equation:

$$D_{SL61}^{meas} = p_{bound} D^{mic} + (1 - p_{bound}) D_{SL61}^{free} \quad (2)$$

where p_{bound} is the fraction of the polymer bound in the micelle, D_{SL61}^{meas} is the measured diffusion coefficient of the polymer in the mixture, D^{mic} is the mixed micelles diffusion coefficient, and D_{SL61}^{free} is the diffusion coefficient of the polymer in the pure solution with 5 mM concentration. If the fraction of surfactant monomers is assumed to be negligible, the measured diffusion coefficient of the two surfactants can be used as a representative for micellar diffusion coefficient. With an average value of 4.67 $\times 10^{-11}$ m^2/s for the micellar diffusion coefficient, $p_{bound} = 0.48$, meaning that only roughly half of the polymer molecules are included in the micelles.

3.5. NOESY Spectra—Structure Investigation of Mixed TX100/SDP2S/SL61 Micelles in the Presence of $AlCl_3$. In order to get a better insight into the origin of the higher oil solubilization capacity of mixed surfactant composition, 2D NOESY spectra[33,34,39−42] were recorded for the TX100/SDP2S, TX100/SL61 and TX100/SDP2S/SL61 systems in the presence of $AlCl_3$, with the aim to determine the mutual arrangement of surfactant molecules in the mixed micelles. Compositions with equal molar fractions of the two surfactants were selected.

The 2D NOESY spectrum (mixing time of 250 ms) of the TX100/SDP2S/SL61 system in the presence of 12 mM $AlCl_3$ is shown in Figure 6. The key cross-peaks indicating the proximity of some intermolecular proton pairs, determinant for unraveling the micelle structure, and supported by build-up curves, are highlighted with arrows.

Only a limited number of resonances could usefully be exploited, because of overlap due to structural similarity of fragments. The most appropriate resonances were the aromatic protons T1 and T2 at 7.11 and 6.76 ppm, and the intense

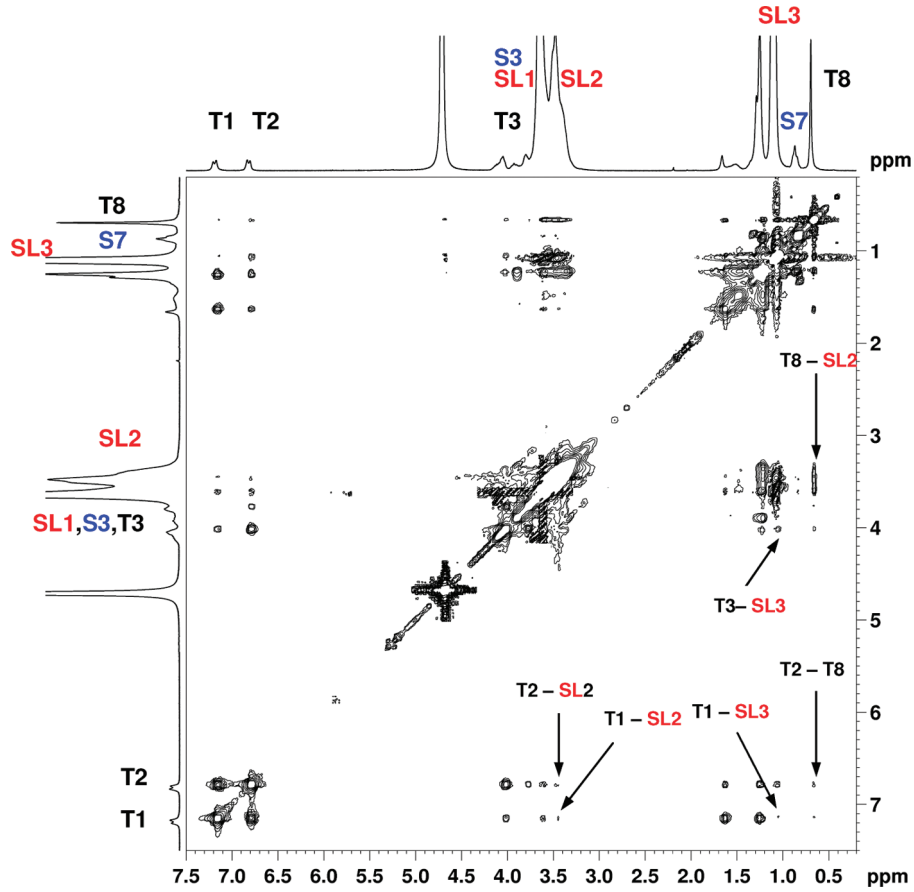

Figure 6. NOESY spectrum (mixing time 250 ms) of the TX100/SDP2S/SL61 system in the presence of 12 mM $AlCl_3$.

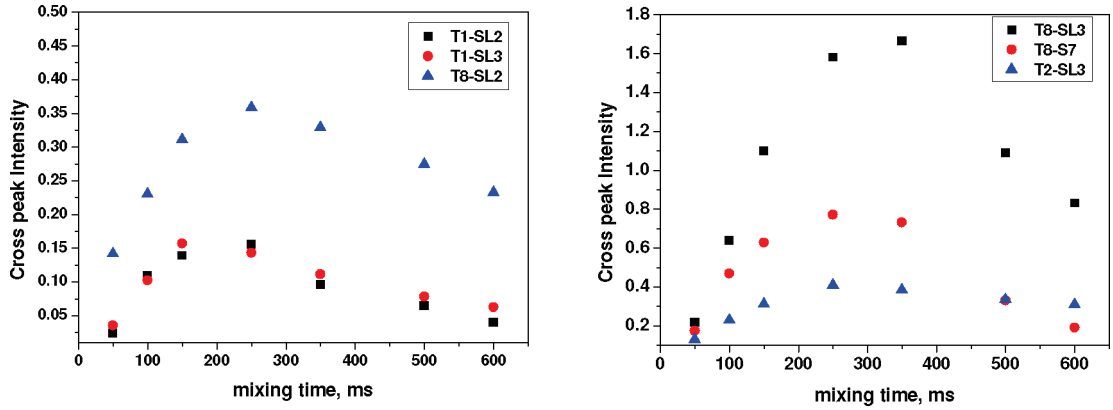

Figure 7. Evolution of some key cross-peak intensities as a function of mixing time in the TX100/SDP2S/SL61/Al^{3+} system.

terminal methyl signal at 0.61 ppm (T8) for TX100, the terminal methyl triplet at 0.78 ppm (S7) for SDP2S, the intense methyl signal at 1.03 ppm (SL3), and the broad methylene resonance at 3.43 ppm (SL2) for SL61.

Our previous structure investigation of pure TX100 solutions showed that, in the low concentration region up to 77.5 mM, individual TX100 micelles are spherical and surfactant molecules form at least two layer structures, with partially overlapping internal and external layers.[34] The NOESY cross-peak patterns of the mixed solutions reveal that the micelles preserve their layer structure as in pure TX100 micelles. This interpretation is confirmed by the key cross-peaks between the terminal methyl resonances (T8) and the T2 aromatic ones, which are also observed in the NOESY spectra of the three TX100/SDP2S, TX100/SL61, and TX100/SDP2S/SL61 mixed micelles and which indicate an intermolecular interaction between these fragments. The NOESY spectra of the two systems with added polymer enable one to conclude that polyoxypropylene fragments of SL61 are incorporated into the micellar core at the level of the inner layer of TX100 molecules, as supported by the T1−SL2, T2−SL2, T6−SL2, and T8−SL2 NOE contacts (see Figures 1 and 6). The additional T1−SL3 and T2−SL3 cross-peaks correlating the aromatic TX100 protons and the methyl group resonances from SL61 also indicate that the polymer is incorporated into the hydrophobic region of the micelle. The T3−SL3 contact suggests that at least some SL3 groups are in contact with the first oxyethylene protons of the outer layer of TX100 molecules. These observations suggest that, owing to its large length, the polyoxypropylene chain tends to coil into the micellar core, while the SL61 polyoxyethylene fragments extend to the micelle periphery where the TX100 polyoxyethylene fragments are located. The NOE T8−S7 cross-peak in mixed TX100/SDP2S and TX100/SDP2S/SL16 indicates spatial proximity between the terminal methyl group from the SDP2S hydrocarbon chain and the terminal *tert*-butyl group of TX100. The lack of further interactions involving S7, with the aromatic TX100 protons T1 and T2, and with any polymer proton (SL2 and/or SL3) suggests that SDP2S molecules are located at the level of the external shell of TX100 molecules.

To eliminate spin-diffusion-related misinterpretations of the observed NOESY correlations, NOE build-up experiments were performed. The key cross-peaks show an initial straight, nearly linear increase with mixing time up to 250−350 ms, safely ruling out spin diffusion. The data are summarized in Figure 7.

A simplified schematic representation of the mixed TX100/SDP2S/SL61 micelle structure in the presence of $AlCl_3$ is proposed in Figure 8.

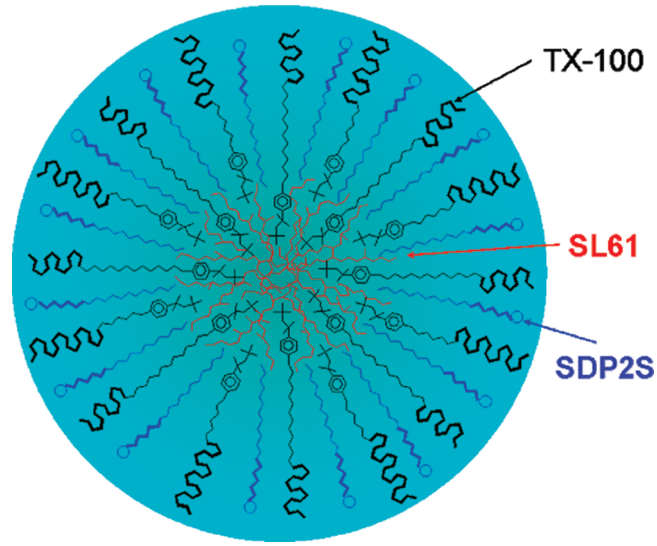

Figure 8. Schematic presentation of mixed TX100/SDP2S/SL61 micelles based on the results from NOESY cross-peaks.

Conclusions

Mixed micellar systems formed by nonionic surfactant TX100, anionic SDP2S and triblock copolymer SL61 were characterized by combining the advantages of DOSY NMR for complex mixture analysis and structural information obtained from NOESY spectra. The results indicate that TX100 is the dominant factor for the micelle formation in mixed TX100/SDP2S systems as long as no $AlCl_3$ is present. By contrast, in the presence of this electrolyte, the anionic surfactant SDP2S is the governing factor for micellar size and shape. The mixed TX100/SDP2S micelles in the presence of both electrolyte and polymer are nearly spherical, with an average radius of 4.5 nm, independent of the micelle composition.

2D NOESY data reveal that mixed TX100/SDP2S/SL61/$AlCl_3$ micelles preserve the TX100 based multilayer structure with partially overlapping external and internal shells of TX100 molecules, with the SDP2S molecules being rather located at the level of the external layer of TX100 molecules, while the polymer is incorporated inside of the micellar core.

Acknowledgment. The financial support by the Fund for Scientific Research-Flanders (FWO, Belgium) for the scientific exchange stay of P.S.D. at the High Resolution NMR Centre of the Vrije Universiteit Brussel (VUB), Belgium, and by the National Science Fund (Grant X-1408), Ministry of Education and Science, Bulgaria, is gratefully acknowledged. P.S.D. and

L.V.L. are indebted to the fund of Scientific Research Flanders (FWO, Belgium) and the Bulgarian Academy of Sciences (BAS) for bilateral scientific exchange fellowships at VUB and BAS (Grant VS.013.07N).

R.W. is indebted to the Fund for Scientific Research-Flanders (FWO, Belgium) for financial support (Grant G.0064.07) and to the Research Council (Onderzoeksraad) of the Vrije Universiteit Brussel for financial support (Concerted Research Action, Grant GOA31 and other grants) of the postdoctoral stay of P.S.D. and the Ph.D. of L.V.L.

References and Notes

(1) Rosen, M.; Murphy, D. *J. Colloid Interface Sci.* **1986**, *110*, 224.
(2) Scamehorn, J. F. In *Phenomena in Mixed Surfactant Systems*; Scamehorn, J. F., Ed.;ACS Symposium Series 311; American Chemical Society: Washington, DC, 1986.
(3) Holland, P. M.; Rubingh, D. N. In *Mixed Surfactant Systems*; ACS Symposium Series 501; American Chemical Society: Washington, DC, 1992.
(4) Palous, J. L.; Turmine, M.; Letellier, P. *J. Phys. Chem. B* **1998**, *102*, 5886.
(5) Rosen, M.; Sulthana, S. *J. Colloid Interface Sci.* **2001**, *239*, 528.
(6) Oliveira, H.; Gehlen, M. *Langmuir* **2002**, *18*, 3792.
(7) Zheng, Y.; Davis, H. *Langmuir* **2000**, *16*, 6453.
(8) Vautier-Giongo, C.; Bakshi, M.; Singh, J.; Ranganathan, R.; Hajdu, J.; Bales, B. *J. Colloid Interface Sci.* **2005**, *282*, 149.
(9) Taboada, P.; Castro, E.; Mosquera, V. *J. Phys. Chem. B* **2005**, *109*, 23760.
(10) Velázquez, M.; Valero, M.; Ortega, F.; González, J. *J. Colloid Interface Sci.* **2007**, *316*, 762.
(11) Sohrabi, B.; Gharibi, H.; Javadian, S.; Hashemianzadeh, M. *J. Phys. Chem. B* **2007**, *111*, 10069.
(12) Schillén, K.; Jansson, J.; Löf, D.; Costa, T. *J. Phys. Chem. B* **2008**, *112*, 5551.
(13) Shrestha, R.; Shrestha, L.; Aramaki, K. *J. Colloid Interface Sci.* **2008**, *322*, 596.
(14) Pettersson, E.; Topgaard, D.; Stilbs, P.; Söderman, O. *Langmuir* **2004**, *20*, 1138.
(15) Fang, X.; Zhao, S.; Mao, S.; Yu, J.; Du, Y. *Colloid Polym. Sci.* **2003**, *281*, 455.
(16) Gouveia, L.; Paillet, S.; Khoukh, A.; Grassl, B.; Müller, A. *Colloids Surf., A* **2008**, *322*, 211.
(17) Jones, M. N.; Gilhooly, E. M.; Nicholas, A. R. *J. Chem. Soc., Faraday Trans.* **1992**, *88*, 2733.
(18) Dubin, P.; Rigsby, R.; McQuigg, D. W. *J. Colloid Interface Sci.* **1985**, *105*, 509.
(19) Dubin, P. L.; Oten, R. *J. Colloid Interface Sci.* **1983**, *95*, 453.
(20) Dubin, P. L.; Oteri, R. *J. Colloid Interface Sci.* **1985**, *13*, 113.
(21) Creeth, A.; Staples, E.; Thompson, L.; Tucker, I.; Penfold, J. *J. Chem. Soc., Faraday Trans.* **1996**, *92*, 589.
(22) Lee, L. T.; Mann, E. K.; Cruselin, D.; Langevin, D.; Farnoux, B.; Penfold, J. *Macromolecules* **1993**, *26*, 7041.
(23) Lima, C. F.; Nome, F.; Zanette, D. *J. Colloid Interface Sci.* **1997**, *189*, 174.
(24) Misselyn-Bauduin, A.; Thibaut, A.; Grandjean, J.; Broze, G.; Jerome, R. *J. Colloid Interface Sci.* **2001**, *238*, 1.
(25) Söderman, O.; Stilbs, P. *Prog. Nucl. Magn. Reson. Spectrosc.* **1994**, *26*, 445–482.
(26) Vangeyte, P.; Leyh, B.; Heinrich, M.; Grandjean, J.; Bourgaux, C.; Jérôme, R. *Langmuir* **2004**, *20*, 8442.
(27) Vangeyte, P.; Leyh, B.; Auvray, L.; Grandjean, J.; Misselyn-Bauduin, A. M.; Jérôme, R. *Langmuir* **2004**, *20*, 9019.
(28) Kralchevsky, P.; Denkov, N. In *Molecular Interfacial Phenomena of Polymers and Biopolymers*; Chen, P., Ed.; Woodhead Publishing: Cambrige, U.K., 2005; Chapter 15, p 538.
(29) Johnson, C. S., Jr. *Prog. Nucl. Magn. Reson. Spectrosc.* **1999**, *34*, 203.
(30) Antalek, B. *Concepts Magn. Reson.* **2002**, *14*, 225.
(31) Lindman, B.; Olsson, U.; Söderman, O. In *Dynamics of Solutions and Fluid Mixtures by NMR*; Delpuech, J., Ed.; Wiley: Chichester, U.K., 1995; Chapter 8.
(32) Söderman, O.; Olsson, U. *Curr. Opin. Colloid Interface Sci.* **1997**, *2*, 131.
(33) Neuhaus, D.; Williamson, M. *The Nuclear Overhauser Effect in Structural and Conformational Analysis*; Wiley-VCH: New York, 2000.
(34) Denkova, P.; Van Lokeren, L.; Verbruggen, I.; Willem, R. *J. Phys. Chem. B* **2008**, *112*, 10935.
(35) Delsuc, M. A.; Malliavin, T. E. *Anal. Chem.* **1998**, *70*, 2146.
(36) Misselyn-Bauduin, A.; Thibaut, A.; Grandjean, J.; Broze, G.; Jerome, R. *Langmuir* **2000**, *16*, 4430.
(37) Alargova, R.; Ivanova, V. P.; Kralchevsky, P. A.; Broze, G.; Mechreteab, A. *Colloids Surf., A* **1998**, *142*, 201.
(38) Alargova, R.; Danov, K. D.; Kralchevsky, P. A.; Broze, G.; Mechreteab, A. *Langmuir* **1998**, *14*, 4036.
(39) Rozycka-Roszak, B.; Cierpicki, T. *J. Colloid Interface Sci.* **1999**, *218*, 529.
(40) Wang, T.; Mao, S.; Miao, X.; Yu, J.; Du, Y. *J. Colloid Interface Sci.* **2001**, *241*, 465.
(41) Yang, X.; Tan, X.; Cheng, G.; Yuan, H.; Mao, S.; Zhao, S.; Yu, J.; Du, Y. *J. Colloid Interface Sci.* **2004**, *279*, 533.
(42) Emin, S. M.; Denkova, P.; Papazova, K. I.; Dushkin, C. D.; Adachi, E. *J. Colloid Interface Sci.* **2007**, *305*, 133.

JP8104369